

Nallathambi Jones Suthan Kissinger

Department of General Studies, Physics Section, Jubail Industrial College, Royal Commission for Jubail, Jubail-10099, Saudi Arabia

Scientific paper

ISSN 0351-9465, E-ISSN 2466-2585

<https://doi.org/10.62638/ZasMat1334>



ZastitaMaterijala 66 (4)  
903 - 912 (2025)

## Studying the sodium effect on the Mo layer by varying the growth pressure on CIGS solar absorption Layer

### ABSTRACT

*Efficiency degradation in flexible Cu(In,Ga)Se (CIGS) solar cells on stainless-steel (STS) substrates occurs due to iron impurity diffusion into the absorber layer. As the primary component of stainless-steel, iron can penetrate the back contact and enter the CIGS absorber, where Fe impurities are known to diminish solar cell performance. In this study, we developed a Sodium doped Molybdenum (Mo-Na) layer as a diffusion barrier on STS substrate using various growth pressures. We examined the Mo-Na diffusion barrier layer using Scanning Electron Microscopy (SEM), X-rdiffractometer (XRD), and Uv-Vis Spectrophotometer. XRD analysis revealed that films grown on STS substrates exhibited a pure chalcopyrite phase with a preferred (112) orientation. We deposited Mo back contact and CIGS layer through co-sputtering and selenization processes, respectively, to investigate Na diffusion through the barrier into the CIGS absorption layer. Secondary ion mass spectroscopy (SIMS) was employed to measure Na and Fe concentrations diffused in the CIGS layer. The SIMS depth profile and optical measurement results clearly showed that Na diffusion into the CIGS absorber layer could be regulated by adjusting the working pressure of the Mo-Na layer. Furthermore, we anticipate significant improvement in CIGS solar cell performance with the Mo-Na diffusion barrier layer, as Na concentration in the CIGS absorption layer affects the efficiency of CIGS solar cells.*

**Keywords:** Flexible Cu(In,Ga)Se<sub>2</sub> (CIGS), Stainless steel, Sputtering, Diffusion barrier, Fe diffusion.

### 1. INTRODUCTION

The quaternary compound Cu(In, Ga)Se (CIGS) is viewed as a promising candidate for high-efficiency, cost-effective photovoltaic cells. CIGS absorber layers demonstrate a notably higher absorption coefficient than silicon. As a well-established thin film solar cell technology, CIGS has reached conversion efficiencies of up to 20.4% in laboratory conditions (1). There is increasing attention on developing solar cell devices on flexible substrates, offering benefits such as adaptable form, decreased weight, and reduced material costs. Incorporating small quantities of sodium (Na) into the p-type absorber layer and its interfaces significantly improves the efficiency of CIGS solar cells (2).

increased open circuit voltage ( $V_{oc}$ ) and fill factor (ff) (3), as well as higher film conductivity due to elevated carrier density (4). However, excessive Na doping can adversely affect cell performance by generating deep defect states that increase recombination (5). Additionally, Na is known to influence the growth characteristics of CIGS.

Recent industrial advancements have led to a significant increase in global production, reaching hundreds of megawatts annually, despite a limited understanding of the material. Opportunities exist to enhance process control and uniformity, potentially reducing the efficiency disparity between small-scale cells and large-scale industrial modules (6). A key industry challenge involves controlling Na diffusion from substrates to the absorber layer. Numerous research groups have investigated Na's effects on CIGS growth (7-11), with conflicting results showing both smaller (12) and larger grains with increased film texturing (13). Various flexible metal substrates are compatible with CIGS solar cells, including stainless steel (STS), titanium, molybdenum, copper, and certain alloys. STS stands out as a particularly viable option due to its

Corresponding author: N. J. Suthan Kissinger

E-mail: [suthanjk@gmail.com](mailto:suthanjk@gmail.com)

Paper received: 01.08.2024.

Paper corrected: 20.12.2024

Paper accepted: 25.12.2024

This enhancement can be attributed to

cost-effectiveness and high mechanical stability. With CIGS being the most promising absorber material, laboratory-scale certified efficiencies have reached 18.7% on polyimide [14] and 17.7% on STS [15] foils. STS substrates offer advantages over polyimide, such as higher temperature stability and tensile strength, allowing CIGS process temperatures up to 600 °C. However, a major drawback of STS substrates is the potential diffusion of iron, its primary component, through the back contact into the CIGS absorption layer, where Fe impurities are known to negatively impact solar cell performance [16]. The main function of incorporating a diffusion barrier layer in CIGS solar cell modules is to prevent impurity diffusion from the metal substrate into the solar cells. Oxide or nitride diffusion barrier layers are commonly employed to inhibit iron diffusion from STS substrates into CIGS absorber layers. These layers should exhibit strong adhesion to STS substrates. Many studies have emphasized the importance of diffusion barriers and Na on STS substrates as impurity blocking layers for

improving solar cell performance [17-19]. However, these barriers may increase production expenses. Our research aims to investigate the impact of growth pressure on the diffusion barrier layer on STS substrates on CIGS-based solar cell properties.

In this study, we investigated the effect growth pressure on the diffusion barrier layer in the flexible CIGS solar cell in terms of the diffusion of metal ions into the CIGS layers. The Molybdenum doped Na diffusion barrier layer is simply formed on STS substrate by annealing the substrate at 600 °C for 1 min under air ambient. The influence and characteristic of the Na concentration diffused from Mo-Na layers was studied by varying the working pressure.

## 2. EXPERIMENTAL PROCEDURE:

We have used commercial stainless-steel (STS) substrates of 25 cm<sup>2</sup> area with a thickness of  $d = 126 \mu\text{m}$ . Table 1 shows the physical properties of the STS substrates.

Table 1. Physical properties of the used stainless steel substrate.

Type	Thickness (um)	$R_a$ (nm)	CTE (ppm K <sup>-1</sup> )	Fe (at%)	Cr (at%)	Mn (at%)	Ni (at%)	C (at%)	Si (at%)
STS 430	126	24.8	10.4	≤82	16-18	≤1.0	≤0.5	≤0.12	≤1.0

Initially, the STS substrates were cleaned by ultra-sonication in acetone and alcohol for 5 min. The iron oxide ( $\alpha\text{-Fe}_2\text{O}_3$ ) diffusion barrier layer was formed on the STS substrate by annealing at 600 °C for 1 min in atmosphere. We varied the annealing time in order to obtain the suitable thickness of  $\alpha\text{-Fe}_2\text{O}_3$  diffusion barrier layers. Subsequently, the Mo back contact and the CIGS absorption layer were grown by sputtering process for investigating the diffusion of impurities into CIGS absorption layer. The Mo back contact layer was consisted of bi-layer structure which was deposited on the  $\alpha\text{-Fe}_2\text{O}_3$  diffusion barrier by DC sputtering in order to obtain an optimal Mo back contact layer. The first layer was deposited at 10 mTorr for a better adhesion and the second layer was subsequently deposited at 3 mTorr for a lower resistivity because the adhesion property was improved when the working pressure was higher. The Molybdenum doped Na diffusion barrier layer is simply formed on STS substrate by annealing the substrate at 600 °C for 1 min under air ambient. Copper indium gallium (CIG) layer was then deposited on the Mo back contact by DC magnetron system using a co-sputtering method with a  $\text{Cu}_{0.8}\text{Ga}_{0.2}$  and anin single

targets. In the selenization process, the CIG precursor was selenized by using the thermal evaporation instrument with the effusion cell. The CIG precursor was converted into CIGS on the absorption layer at 500 °C for an hour to form the p-type CIGS chalcopyrite structure. The schematic representation of different process involved is shown in Figure 1.

The X-ray diffraction (XRD) measurement of the CIGS solar cells was performed by using a Rigakudiffractometer with  $\text{Cu K}\alpha$  radiation. The grown Mo-Na nano layers deposited for various working pressure were characterized by field-emission scanning electron microscopy (FE-SEM) and Energy Dispersive X-ray Spectroscopy (EDX). The surface of STS substrate annealed at 600 °C for 1 min was identified by Raman spectroscopy. The thickness of the diffusion barrier was observed by using transmission electron microscopy (TEM) analysis. The depth profile was analyzed by secondary ion mass spectroscopy (SIMS) system (CAMECA IMS 7f magnetic sector) with  $\text{Cs}^+$  source ions (10 kV, current 30 nA) for Na and Fe diffused from STS substrate.

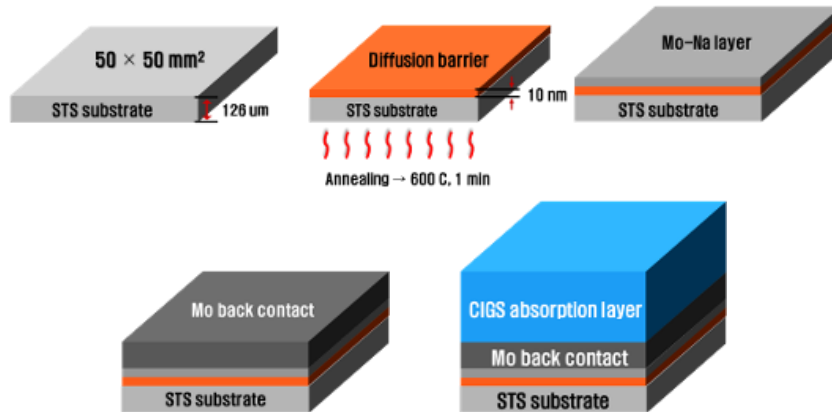


Figure 1. Schematic representation of different process involved in the growth of CIGS absorption layer for various growth pressures

### 3. RESULTS AND DISCUSSION

FESEM was employed to examine the surface morphology and cross-section of Mo-Na Layer

deposited at various working pressures. Figure 2 displays the planar and cross-sectional FESEM images of the Mo-Na layer at different working pressures.

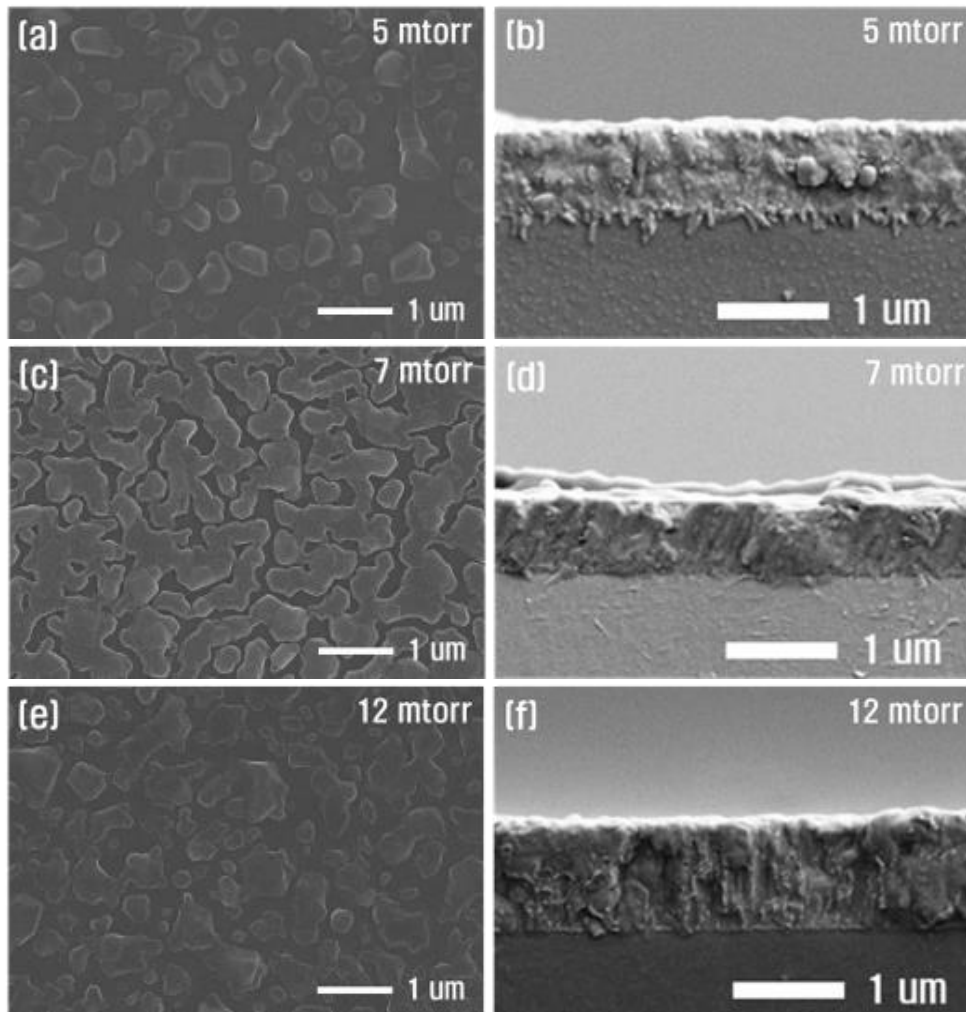


Figure 2. Plane & cross-sectional FE-SEM images of Mo-Na layers grown at (a), (b) 5 mtorr, (c), (d) 7 mtorr, (e), (f) 12 mtorr

Cross-sectional views reveal that all films exhibit a columnar grain structure. Films deposited at high pressure demonstrate greater density with closed grain boundaries, while those at low pressure show less density with more open grain boundaries. Top-view images indicate larger grain sizes for 12.00 torr compared to other samples. Pressures exceeding 12.00 torr resulted in notably different grain microstructures due to high Na content in the layer. Other research groups (20-22) also observed grain size changes in CIGS absorber layers with high Na concentrations and various Na incorporation methods. The morphological changes in Mo-Na

layers suggest that Na is supplied from Na-doped Mo, with its quantity regulated by different working pressures. EDX measurements, presented in Figure 3, characterize the atomic concentrations on the Mo-Na layer surface and within the layer. Fig. 3 (a) clearly shows that the atomic concentration of Na on the Mo-Na layer surface exceeded that within the layer. This indicates that the amount of Na diffused from the Mo-Na layer could be controlled by working pressure, demonstrating that Na diffusion is strongly influenced by the Mo-Na layer's microstructure. Table 2 presents the atomic concentration levels of Na, Mo, and O in the top and bottom layers, as determined by EDX analysis.

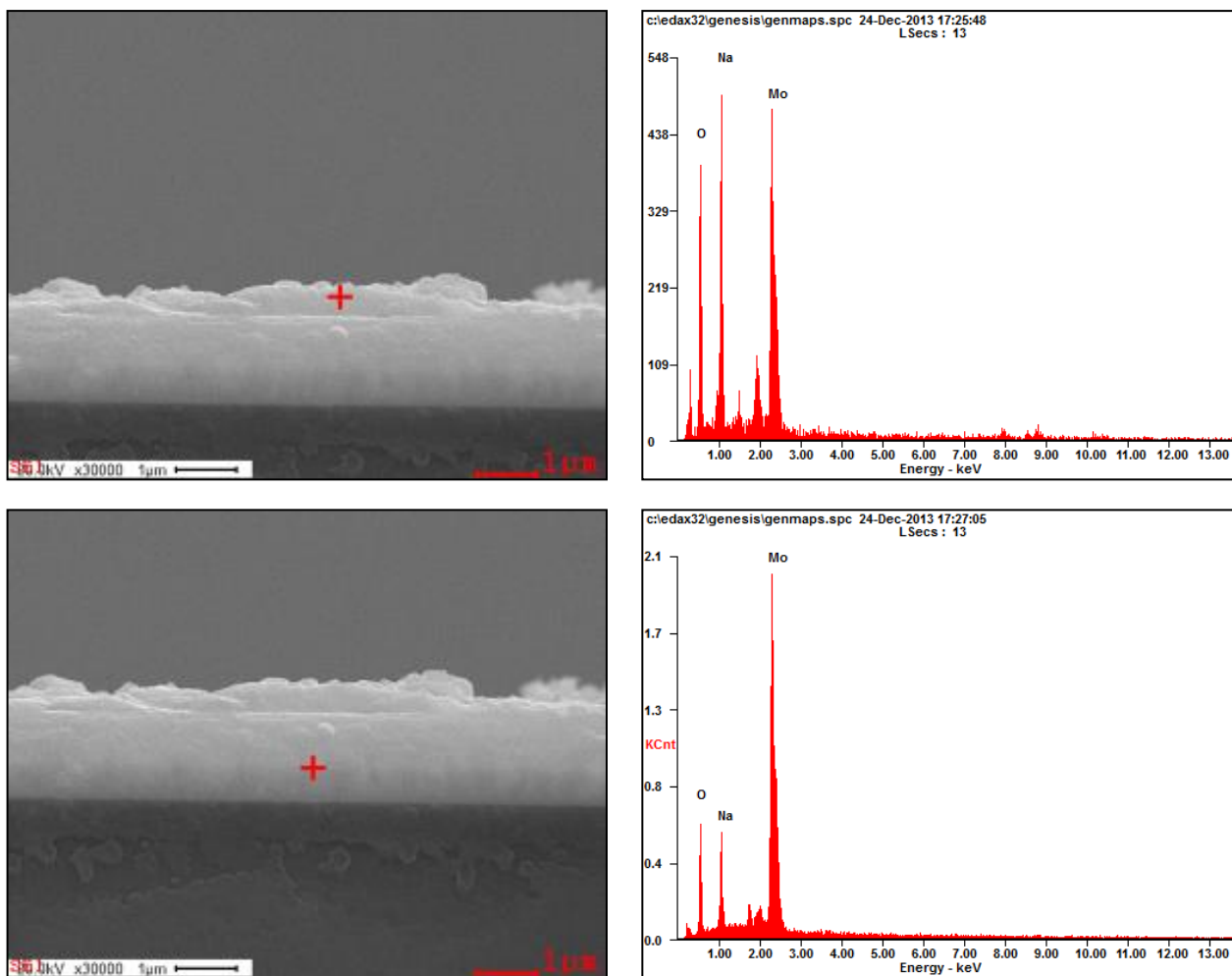


Figure 3. The atomic concentration of (a) surface on Mo-Na layer and (b) Mo-Na layer by EDX

Table 2: Atomic concentration levels of Na, Mo and O by EDX analysis

	Atomic % Na	Atomic % Mo	Atomic % O
Top Layer	65.64	32.77	1.58
Bottom Layer	11.87	7284	15.28

Figure 4 illustrates the SIMS depth profile of sodium concentration in CIGS absorber layers on Mo/Mo-Na substrates at various growth pressures. The sodium distribution is generally uniform across the region for most growth pressures, with the exception of high pressures. Sodium levels fluctuated with deposition pressure and depth,

reaching their lowest point in the middle. The diffusion levels and distributions of sodium in the Mo-Na back contact layer are comparable to those shown in Figure 5, suggesting that Mo-Na deposited at low pressure contains notably less sodium than that deposited at high pressure. Despite these variations, sodium levels in the three absorber layers appear consistent, regardless of the

underlying Mo-Na layer. All samples exhibit significant sodium accumulation on CIGS surfaces. This suggests that a sodium-doped Mo layer can be readily incorporated into the CIGS production process, potentially offering greater effectiveness for CIGS cells on flexible substrates such as stainless steel, titanium, or polymer.

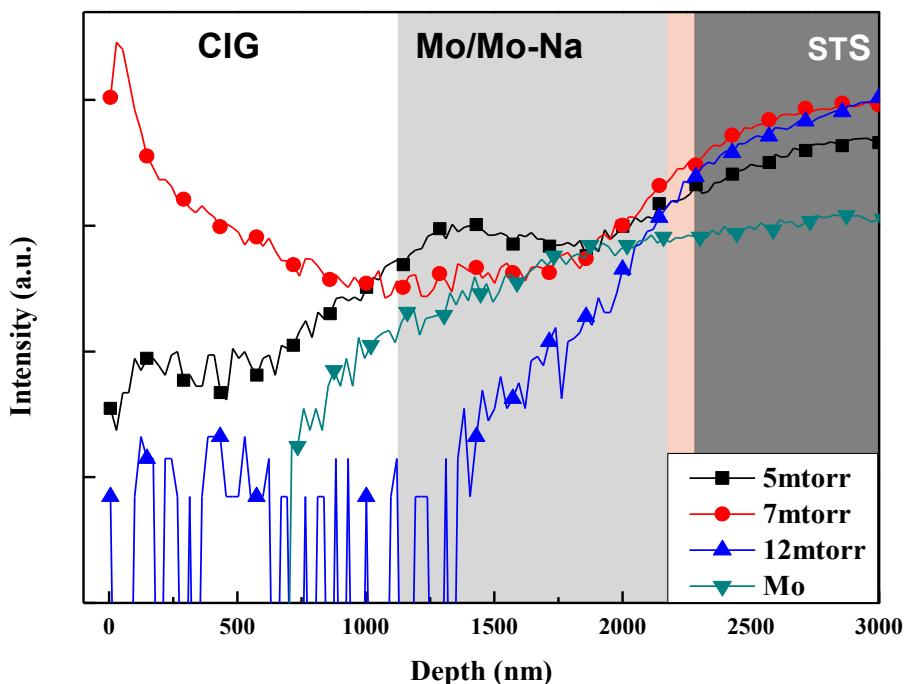


Figure 4. SIMS depth profile for Na concentration in CIGS absorption layer with Mo/Mo-Na layer

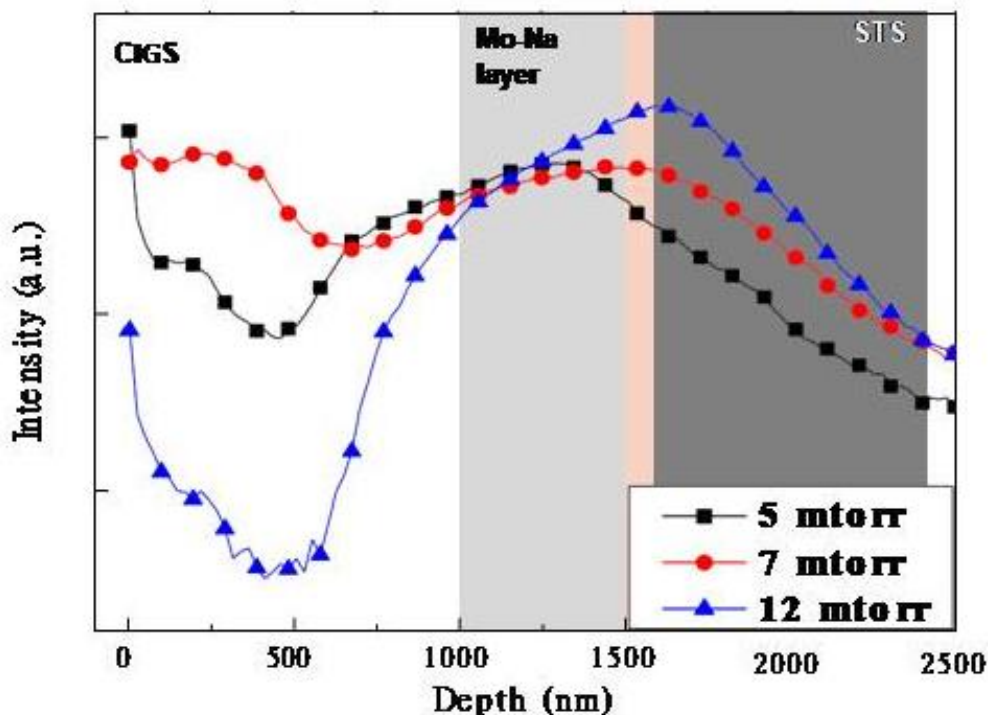


Figure 5. SIMS depth profile for Na concentration in CIGS absorption layer

CuInGa (CIG) precursor layers were deposited on Mo/Mo-Na/ $\alpha$ -Fe<sub>2</sub>O<sub>3</sub> diffusion barrier/STS substrates using co-sputtering techniques. These layers were then transformed into CIGS absorption layers through selenization at 500 °C for one hour to examine the impact of Fe impurities from the STS substrate. SIMS data in Figure 6 demonstrates that the  $\alpha$ -Fe<sub>2</sub>O<sub>3</sub> diffusion barrier, created by annealing the STS substrate, effectively impedes impurity diffusion. With identical gradients, the influence of impurity diffusion on CIGS solar cells with an  $\alpha$ -Fe<sub>2</sub>O<sub>3</sub> barrier layer can be easily compared. The

trace element profiles of Fe and Cr differ significantly among samples. Without a diffusion barrier, numerous Fe impurities migrated from the STS substrate into the CIGS absorption layer. In the absence of an  $\alpha$ -Fe<sub>2</sub>O<sub>3</sub> barrier, most Fe ions remained within the absorber layer. High Fe signal intensities in the CIGS absorption layer indicate substantial Fe atom diffusion from the STS substrate. The SIMS depth profile reveals that the  $\alpha$ -Fe<sub>2</sub>O<sub>3</sub> diffusion barrier significantly reduced impurity diffusion from the STS substrate and may enhance CIGS solar cell performance.

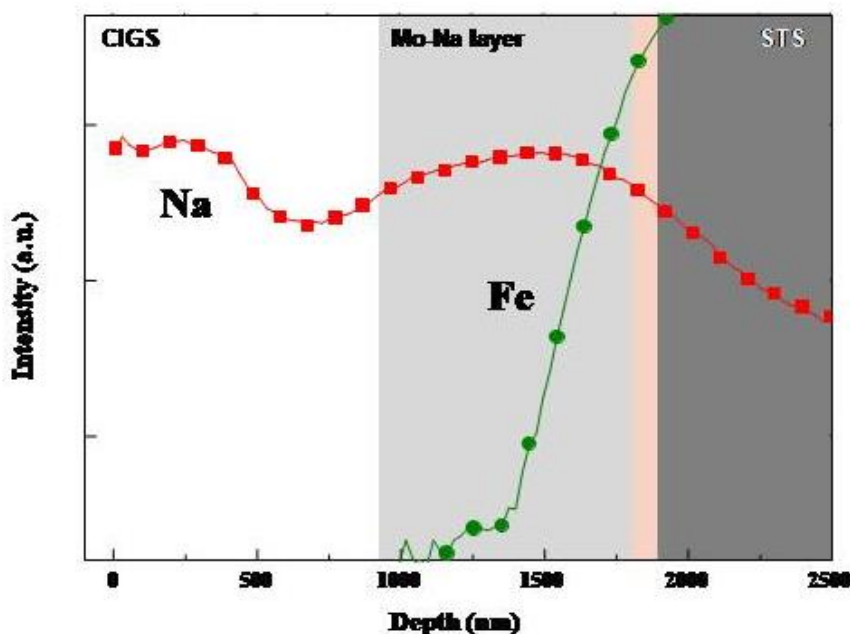


Figure 6. SIMS depth profile for Fe & Na concentration in CIGS absorption layer with various Mo-Na layer

The SIMS depth profile of Na concentration in CIGS absorber layers on Mo/Mo-Na substrates at various growth pressures is shown in Figure 4. Na distribution is generally uniform across the region for all growth pressures, except at high pressures. Na levels varied with deposition pressure and depth, reaching their minimum in the middle. The diffusion levels and distributions of Na in the Mo-Na back contact layer are similar to those in Figure 5, indicating that Mo-Na deposited at low pressure contains significantly less Na than that deposited at high pressure. Despite these differences, Na levels in the three absorber layers seem consistent, regardless of the underlying Mo-Na layer. All samples show substantial Na accumulation on CIGS surfaces. This indicates that a Na-doped Mo layer can be easily integrated into the CIGS production process, potentially offering greater efficacy for CIGS cells on flexible substrates like stainless steel, Ti, or polymer.

The phase structures of CIGS solar cells module on STS substrate were examined using XRD analysis. Figure 7 displays the XRD diffractograms of the CIGS solar cell structure at various growth pressures on the STS substrate. The XRD data clearly demonstrates the effect of growth pressure on the Na doped Mo layer. The CIGS structure exhibited prominent diffraction peaks at  $2\theta$  values of 27, 44 and 53°, corresponding to the (112), (220) and (116/312) planes (JCPDS-#35-1102). All identified peaks belonged to the CIGS chalcopyrite phase, with no secondary phases detected. As the working pressure increased, the (112) peak position shifted towards higher  $2\theta$  values. Additionally, impurity-related diffraction peaks appeared at  $2\theta$  values of 44.5, 65 and 82.5°. The introduction of an  $\alpha$ -Fe<sub>2</sub>O<sub>3</sub> diffusion barrier layer in the CIGS solar cell structure significantly reduced the impurity levels of Fe, Ni and Cr. These findings indicate that the growth pressure of the CIGS layer deposited on the Mo-Na layer on the STS substrate significantly

influences the structural properties of the CIGS solar cell module. Furthermore, varying the growth pressure of the Mo-Na layer enhanced the crystallinity of the CIGS absorption layer. It is

believed that adjusting the growth pressures of the Mo-Na layer in the CIGS solar structure can enhance device performance.

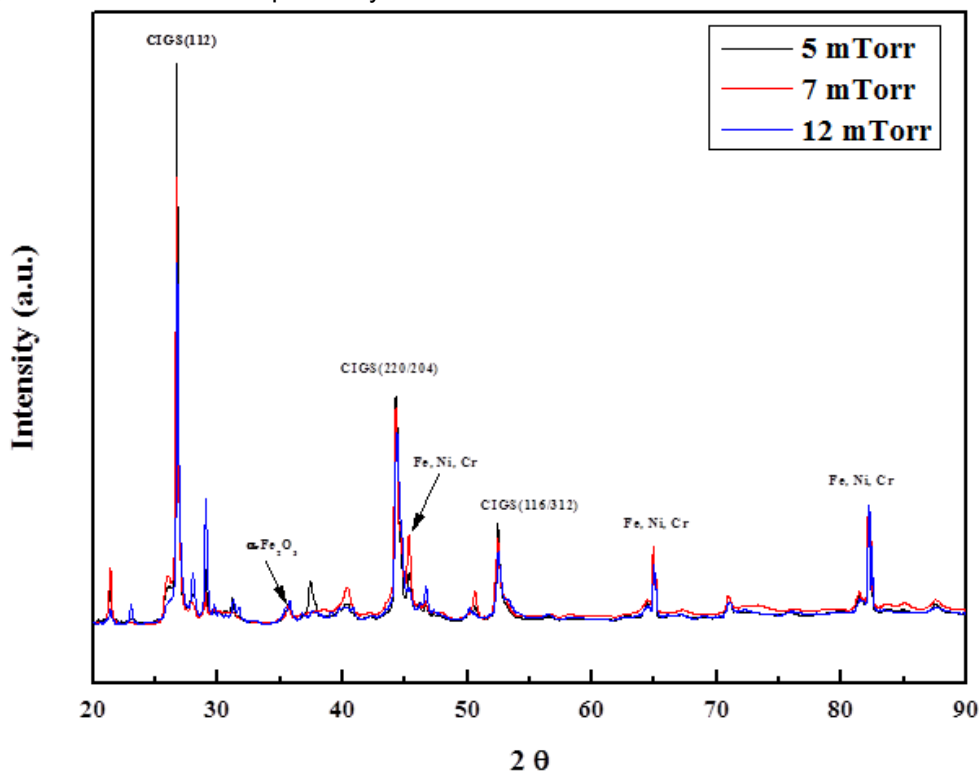


Figure 7. X-ray diffraction patterns of CIGS absorption layer with various Mo-Na layers

The mean crystallite size of polycrystalline CIGS thin films can be estimated by Scherrer Eq. (22):

$$D = \frac{K\lambda}{\beta \cos\theta} \tag{1}$$

Where  $D$  is the mean crystallite size,  $\lambda$  is the x-ray wave length ( $\lambda = 1.54 \text{ \AA}$  for  $\text{CuK}\alpha$  radiation),  $\beta$  is the full width half maximum (FWHM),  $\theta$  is the Bragg angle, and  $K$  is the shape factor. The calculated crystalline size were in the range of 60-100 nm.

The dependence of optical bandgap ( $E_g$ ) on various working pressures was studied using the optical data, including transmittance and reflectance spectra acquired from CIGS absorption layer on Mo/Mo-Na layer. The optical absorption coefficient,  $\alpha$ , was calculated using the following equation:

$$\alpha = \frac{1}{d} \ln \left[ \frac{\sqrt{(1-R)^4 + 4T^2R^2} + (1-R)^2}{2T} \right] \tag{2}$$

Where  $d$  is the film thickness,  $R$  is the reflectance, and  $T$  is the transmittance. Since chalcogenide

compounds are direct gap semiconductors (22), the following equation can be used (24).

$$\alpha h\nu = A_a (h\nu - E_g)^{1/2} \tag{3}$$

Where  $A_a$  is a constant that depends on the transition nature, the effective mass and the refractive index, and  $h\nu$  is the incident photon energy. The bandgap was then determined by extrapolating the linear portion of  $(\alpha h\nu)^2$  versus  $h\nu$  curve to the abscissa.

Figure 8 shows the plot of  $(\alpha h\nu)^2$  versus  $h\nu$  which was plotted in the wavelength range of 800 – 1200 nm for the CIGS solar cell structure for different growth pressures. The extrapolation of the tangential line to these plots to zero absorption can provide the appropriate values of the band gap energy of the CIGS solar cell structure with Mo-Na layer. The optical bandgap energies of the CIGS solar cell structure for various growth pressures were estimated to be 1.00, 1.06, and 0.97 eV, respectively. It was noted that the bandgap of CIGS absorption layer was increased by increasing Na concentration diffused from the Mo-Na layer.

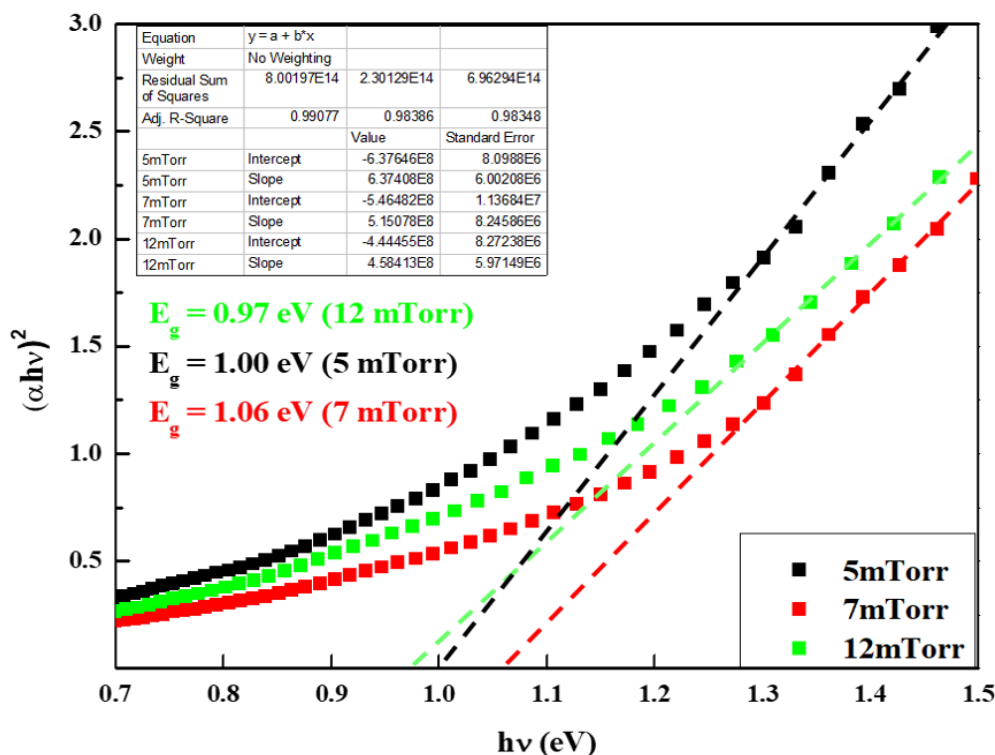


Figure 8. Optical bandgap of CIGS absorption layer with various Mo-Na layers

#### 4. CONCLUSION

The attainment of high-efficiency CIGS thin film solar cells heavily relies on sodium diffusion from the substrate. However, regulating sodium diffusion from soda-lime glass, a common and widely utilized sodium source, presents challenges. Furthermore, CIGS cells with sodium-free substrates require the deposition of additional sodium source material. In this study, we examined how working pressure affects the characteristics of Mo-Na layers deposited on stainless steel substrates using an in-line DC magnetron sputtering system. Our findings revealed that working pressure is a crucial factor in producing high-performance CIGS solar cell modules. XRD analysis confirmed that the films exhibited appropriate composition and structure with good crystallinity. The Mo-Na layer's microstructure was identified as a critical factor for sodium diffusion, with layers sputtered at high pressure demonstrating improved sodium out-diffusion performance. As the working pressure increased from 5mTorr to 12mTorr, the optical bandgap of each film, determined through transmittance and reflectance spectra, rose from 0.97 to 1.06 eV. Our research shows that by manipulating the growth pressure of the Mo-Na layer, sodium can be effectively incorporated into the CIGS absorber layer.

#### 5. REFERENCES

- [1] P. ReinhardChirila, F. Pianezzi, P. Bloesch, A.R. Uhl, C. Fella, L.Kranz, D. Keller, C. Gretener, H. Hagendorfer, D. Jaeger, R. Erni, S. Nishiwaki, S. Buecheler, A.N. Tiwari (2013) Potassium-induced surface modification of Cu(In,Ga)Se<sub>2</sub> thin films for high-efficiency solar cells. *Nat. Mater.* 12, 1107-1111, <https://doi.org/10.1038/nmat3789>.
- [2] J.E. Granata, J.R. Sites, S. Asher, R.J. Matson (1997) Quantitative incorporation of sodium in CuInSe<sub>2</sub> and Cu(In,Ga)Se<sub>2</sub> photovoltaic devices. *Proceedings of the Conference Record of 26Th IEEE Photovoltaic Specialists Conference*, p.387-390, <https://doi.org/10.1109/PVSC.1997.654109>.
- [3] Y. Sakurai, A. Yamada, P. Fons, K. Matsubara, T. Kojima, S. Niki, T. Baba, T. Tsuchimochi, Y. Kimura, Nakanishi (2003) Adjusting the Sodium diffusion into CuInGaSe<sub>2</sub> absorbers by preheating of Mo/SLG substrates. *J. Phys. Chem. Solids*, 64, 1877-1880, [https://doi.org/10.1016/S0022-3697\(03\)00173-2](https://doi.org/10.1016/S0022-3697(03)00173-2).
- [4] F. Kessler, D. Rudmann (2004) Technological effects of flexible CIGS solar cells and modules. *Sol Energy*, 77, 685-695, <https://doi.org/10.1016/j.solener.2004.04.010>.
- [5] S.H. Wei, S.B. Zhang, A. Zunger (1999) Effects of Na on the electrical and structural properties of CuInSe<sub>2</sub>. *J. Appl. Phys.*, 85, 7214-7218, <https://doi.org/10.1063/1.370534>.
- [6] E. Wallin, U. Malm, T. Jarmar, O. Lundberg, M. Edoff, and L. Stolt (2012) World-record Cu(In,Ga)Se<sub>2</sub>-

- based thin-film sub-module with 17.4% efficiency. *Prog. Photovoltaics: Res. Appl.*, 20, 851-854, <https://doi.org/10.1002/pip.2246>.
- [7] M. Bodegard, K. Granath, L. Stolt (2000) Growth of Cu(In,Ga)Se<sub>2</sub> thin films by coevaporation using alkaline precursors. *Thin Solid Films*, 361-362, 1-16, [https://doi.org/10.1016/S0040-6090\(99\)00828-7](https://doi.org/10.1016/S0040-6090(99)00828-7).
- [8] D. Rudmann, A.F. Da Cunha, M. Kaelin, F. Kurdesau, H. Zogg, A.N. Tiwari, G. Bilger (2004) Efficiency enhancement of Cu(In,Ga)Se<sub>2</sub> solar cells due to post-deposition Na incorporation. *Appl. Phys. Lett.*, 84, 1129-1131, <https://doi.org/10.1063/1.1646758>
- [9] D.W. Niles, K. Ramanathan, F. Hasoon, R. Noufi, B.J. Tielsch, and J.E. Fulghum (1997) Na impurity chemistry in photovoltaic CIGS thin films: Investigation with x-ray photoelectron spectroscopy. *J. Vac. Sci. Technol. A*, 15, 3044-3049, <https://doi.org/10.1116/1.580902>.
- [10] X. Song, R. Caballero, R. Felix, D. Gerlach, C.A. Kaufmann, H.-W. Schock, R.G. Wilks, M. Bar (2012) Na incorporation into Cu(In,Ga)S<sub>2</sub> thin-film solar cells absorbers deposited on polyimide: Impact on the chemical and electronic surface structure. *J. Appl. Phys.*, 111, 034903-1-034903, <https://doi.org/10.1063/1.3679604>.
- [11] D.J. Schroeder, A.A. Rockett (1997) Electronic effects of sodium in epitaxial CuIn<sub>1-x</sub>Ga<sub>x</sub>Se<sub>2</sub>. *J. Appl. Phys.*, 82, 4982-2985, <https://doi.org/10.1063/1.366365>.
- [12] M. Ruckh, D. Schmid, M. Kaiser, R. Schiffler, T. Walter, H.W. Schock (1996) Influence of substrates on the electrical properties of Cu(In,Ga)Se<sub>2</sub> thin films. *Solar Energy Mater. Solar Cells*, 41-42, 335-434, [https://doi.org/10.1016/0927-0248\(95\)00105-0](https://doi.org/10.1016/0927-0248(95)00105-0).
- [13] R. Kaigawa, Y. Satake, K. Ban, S. Merdes, R. Klenk (2011) Effects of Na on the properties of Cu(In,Ga)S<sub>2</sub> Solar Cells. *Thin Solid Films*, 516, 16, 5535-5538, <https://doi.org/10.1016/j.tsf.2011.02.044>.
- [14] F. Pianezzi, A. Chirila, P. Blosch, S. Seyrling, S. Buecheler, L. Kranz, C. Fella, A.N. Tiwari (2010) Electronic properties of Cu(In,Ga)Se<sub>2</sub> solar cells on stainless steel foils without diffusion barrier. *Prog. Photovolt. Res. Appl.*, 20, 253, <https://doi.org/10.1002/pip.1247>.
- [15] P. Jackson, D. Hariskos, E. Lotter, S. Paetel, R. Wuerz, R. Menner, W. Wischmann, M. Powalla (2011) New world record efficiency for Cu(In,Ga)Se<sub>2</sub> thin-film solar cells beyond 20%. *Prog. Photovolt. Res. Appl.*, 19, 894, <https://doi.org/10.1002/pip.1078>.
- [16] P. Jackson, P. Grabitz, A. Strohm, G. Bilger, H. W. Schock (2004) Contamination of Cu(In,Ga)Se<sub>2</sub> solar cells by metallic substrate elements. *Proceedings of the 19<sup>th</sup> European Photovoltaic Solar Energy Conference*, 1936-1938.
- [17] C. P. Bjorkman, S. Jani, J. Westlinder, M. K. Linnarsson, J. Scragg, M. Edoff (2013) Diffusion of Fe and Na in co-evaporated Cu(In,Ga)Se<sub>2</sub> devices on steel substrates. *Thin Solid Films*, 535, 188-192, <https://doi.org/10.1016/j.tsf.2012.11.067>.
- [18] D. Bae, S. Kwon, J. Oh, W. K. Kim, H. Park (2013) Investigation of Al<sub>2</sub>O<sub>3</sub> diffusion barrier layer fabricated by atomic layer deposition for flexible Cu(In,Ga)Se<sub>2</sub> solar cells. *Renewable Energy*, 55, 62-68, <https://doi.org/10.1016/j.renene.2012.12.024>.
- [19] K. Herz, F. Kessler, R. Wachter, M. Powalla, J. Schneider, A. Schulz, and U. Schumacher (2002) Dielectric barriers for flexible CIGS solar modules. *Thin Solid Films*, 403-404, 84 - 389, [https://doi.org/10.1016/S0040-6090\(01\)01516-4](https://doi.org/10.1016/S0040-6090(01)01516-4).
- [20] D. Rudmann, G. Bilger, M. Kaelin, F.-J. Haug, H. Zogg, A.N. Tiwari (2003) Effects of NaF coevaporation on structural properties of Cu(In,Ga)Se<sub>2</sub> thin films. *Thin Solid Films*, 421-432, 37-40, [https://doi.org/10.1016/S0040-6090\(03\)00246-3](https://doi.org/10.1016/S0040-6090(03)00246-3).
- [21] S. Ye, X. Tan, M. Jiang, B. Fan, K. Tang, S. Zhuang (2010) Impact of different Na incorporating methods on Cu(In,Ga)Se<sub>2</sub> thin film solar cells with a low-Na substrate. *Appl. Opt.*, 49, 1662-1665, <https://doi.org/10.1364/AO.49.001662>.
- [22] J.H. Yun, K.H. Kim, M. Kim, B.T. Ahn, S.J. Ahn, J.C. Lee, K.H. Yoon (2007) Fabrication of CIGS solar cells with a Na-doped Mo layer on a Na-free substrate. *Thin Solid Films*, 515, 5876-5879, <https://doi.org/10.1016/j.tsf.2006.12.156>.
- [23] C. Chuan Chen, X. Qi, M.G. Tsai, Y.F. Wu, I.G. Chen, C.Y. Lin, P.H. Wu, K.P. Chang (2013) Low-temperature growth of Na doped CIGS films on flexible polymer substrates by pulsed laser ablation from a Na containing target. *Surface and Coatings Technology*, 231, 209-213, <https://doi.org/10.1016/j.surfcoat.2012.06.065>.
- [24] J. Parravicini, M. Acciarri, M. Murabito, A.L. Donne, A. Gasparotto, S. Binetti (2018) In-depth photoluminescence spectra of pure CIGS thin films. *Appl. Opt.*, 57, 1849-1856, <https://doi.org/10.1364/AO.57.001849>.

## IZVOD

### PROUČAVANJE EFEKTA Natrijuma u sloju Mo u variranju pritiska rasta na CIGS solarnom apsorpcionom sloju

Smanjenje efikasnosti u fleksibilnim Cu(In,Ga)Se (CIGS) solarnim ćelijama na podlogama od nerđajućeg čelika (STS) nastaje usled difuzije nečistoća gvožđa u sloj apsorbera. Kao primarna komponenta nerđajućeg čelika, gvožđe može da proдре u zadnji kontakt i uđe u CIGS apsorber, gde je poznato da nečistoće Fe smanjuju performanse solarnih ćelija. U ovoj studiji razvili smo sloj molibdena dopiranog natrijumom (Mo-Na) kao difuzionu barijeru na STS supstratu koristeći različite pritiske rasta. Ispitali smo sloj Mo-Na difuzione barijere korišćenjem skenirajuće elektronske mikroskopije (SEM), Ks-rdifraktometra (KSRD) i Uv-Vis spektrofotometra. KSRD analiza je otkrila da filmovi uzgojeni na STS supstratima pokazuju čistu halkopiritnu fazu sa preferiranom (112) orijentacijom. Naneli smo Mo povratni kontakt i CIGS sloj kroz procese ko-prskanja i selenizacije, respektivno, da bismo istražili difuziju Na kroz barijeru u CIGS apsorpcioni sloj. Sekundarna jonska masena spektroskopija (SIMS) je korišćena za merenje koncentracija Na i Fe difuznih u CIGS sloju. SIMS profil dubine i rezultati optičkog merenja jasno su pokazali da se difuzija Na u sloj apsorbera CIGS može regulisati podešavanjem radnog pritiska Mo-Na sloja. Štaviše, očekujemo značajno poboljšanje performansi CIGS solarnih ćelija sa slojem barijere za difuziju Mo-Na, pošto koncentracija Na u CIGS apsorpcionom sloju utiče na efikasnost CIGS solarnih ćelija.

**Ključne reči:** Fleksibilni Cu(In,Ga)Se<sub>2</sub> (CIGS), nerđajući čelik, raspršivanje, difuziona barijera, Fe difuzija.

Naučni rad

Rad primljen: 01.08.2024.

Rad korigovan: 20.12.2024.

Rad prihvaćen: 25.12.2024.

Nallathambi Jones Suthan Kissinger: <https://orcid.org/0000-0002-6866-5282>